Optical constants of $Ga_{1-x}In_xAs_ySb_{1-y}$ lattice matched to GaSb (001): Experiment and modeling

M. Muñoz,[a] K. Wei, and Fred H. Pollak[b]
Physics Department and New York State Center for Advanced Technology in Ultrafast Photonic Materials and Applications, Brooklyn College of the City University of New York, Brooklyn, New York 11210

J. L. Freeouf
Interface Studies, Inc., Katonah, New York 10536

C. A. Wang
Lincoln Laboratory, Massachusetts Institute of Technology, Lexington, Massachusetts 02420-9108

G. W. Charache
Lockheed Martin Corporation, Schenectady, New York 12301

(Received 19 July 1999; accepted for publication 4 November 1999)

The optical constants $\epsilon(E)[=\epsilon_1(E)+i\epsilon_2(E)]$ of two epitaxial layers of GaInAsSb/GaSb have been measured at 300 K using spectral ellipsometry in the range of 0.35–5.3 eV. The $\epsilon(E)$ spectra displayed distinct structures associated with critical points (CPs) at E_0 (direct gap), spin-orbit split $E_0+\Delta_0$ component, spin-orbit split $(E_1,E_1+\Delta_1)$ and $(E_0',E_0'+\Delta_0')$ doublets, as well as E_2. The experimental data over the entire measured spectral range (after oxide removal) has been fit using the Holden model dielectric function [Holden *et al.*, Phys. Rev. B **56**, 4037 (1997)] based on the electronic energy-band structure near these CPs plus excitonic and band-to-band Coulomb-enhancement effects at E_0, $E_0+\Delta_0$, and the E_1, $E_1+\Delta_1$ doublet. In addition to evaluating the energies of these various band-to-band CPs, information about the binding energy (R_1) of the two-dimensional exciton related to the E_1, $E_1+\Delta_1$ CPs was obtained. The value of R_1 was in good agreement with effective mass/$\mathbf{k}\cdot\mathbf{p}$ theory. The ability to evaluate R_1 has important ramifications for recent first-principles band-structure calculations which include exciton effects at E_0, E_1, and E_2 [M. Rohlfing and S. G. Louie, Phys. Rev. Lett. **81**, 2312 (1998); S. Albrecht *et al.*, Phys. Rev. Lett. **80**, 4510 (1998)]. The experimental absorption coefficients in the region of E_0 were in good agreement with values obtained from a linear interpolation of the end-point materials. Our experimental results were compared to a recent evaluation and fitting (Holden model) of the optical constants of GaSb. © *2000 American Institute of Physics.* [S0021-8979(00)04004-4]

I. INTRODUCTION

The quaternary alloy $Ga_{1-x}In_xAs_ySb_{1-y}$ lattice matched to GaSb is a narrow-band-gap semiconductor (0.3–0.7 eV) with a number of applications including thermophotovoltaic cells,[1] infrared light-emitting diodes[2] and lasers,[3–8] and photodetectors.[9,10] The optical constants are of interest for fundamental reasons as well as for these applications. However, in spite of its significance, relatively little work has been reported on the optical properties related to the electronic band structure. Snyder *et al.* have used a Fourier transform infrared variable angle spectral ellipsometer in the range of 0.089–0.620 eV to investigate undoped and Te-doped $Ga_{0.85}In_{0.15}As_{0.17}Sb_{0.83}$ epilayers lattice matched to GaSb.[11] The onset of the band gap at about 0.55 eV was observed for the undoped sample. The data below the band gap for the doped material displayed free-carrier as well as interference effects. Measurements of the complex dielectric function $\epsilon(E)[=\epsilon_1(E)+i\epsilon_2(E)]$ for a doped sample also were reported in the range 0.7–5.4 eV using a rotating analyzer spectral ellipsometer.[11] Investigations of the reflectivity in the infrared have been reported by Mezerreg *et al.* (25–250 μm) (Ref. 12) and Belov *et al.* (20–260 μm).[13]

In this article we report a room-temperature spectral ellipsometry (SE) investigation of the complex dielectric function $\epsilon(E)$ of two $Ga_{1-x}In_xAs_ySb_{1-y}$/GaSb samples [sample Nos. 1 $(x=0.16,y=0.14)$ and 2 $(x=0.15,y=0.14)$] in the photon energy range of 0.35–5.3 eV. Distinct structures associated with critical points (CPs) at E_0 (direct gap), spin-orbit split $E_0+\Delta_0$ component, spin-orbit split $(E_1,E_1+\Delta_1)$ and $(E_0',E_0'+\Delta_0')$ doublets, as well as E_2 were observed. The experimental data over the entire measured spectral range (after oxide removal) have been fit using the Holden model dielectric function[14–17] based on the electronic energy-band structure near these CPs plus the discrete and continuum excitonic effects at E_0, $E_0+\Delta_0$, E_1, and $E_1+\Delta_1$. The $E_0',E_0'+\Delta_0'$ structures were also included in the analysis. In addition to evaluating the energies of these various band-to-band CPs, it is possible to obtain information about the binding energy (R_1) of the two-dimensional (2D) exciton related to the $E_1,E_1+\Delta_1$ CPs. The obtained value of

[a]Permanent address: Departamento de Fisica; CINVESTAV-IPN; Mexico DF, Mexico, electronic mail: martin@fis.cinvestav.mx.
[b]Also at the Graduate School and University Center of the City University of New York, New York, NY 10036, electronic mail: fhpbc@cunyvm.cuny.edu

 © 2000 American Institute of Physics

R_1 is in reasonable agreement with effective mass/$\mathbf{k}\cdot p$ theory.[18] The ability to evaluate R_1 has important ramifications for recent first-principles band-structure calculations which include exciton effects at E_0, E_1, and E_2.[19,20] The experimental absorption coefficients in the region of E_0 were in good agreement with values obtained from a linear interpolation of the end-point materials. Our results were compared with a recent room-temperature SE investigation of the optical constants of single-crystal GaSb.[17] We also performed room-temperature photoluminescence (PL) to evaluate the fundamental band gap.

II. EXPERIMENTAL DETAILS

The two samples consisted of epitaxial layers fabricated by organometallic vapor-phase epitaxy (OMVPE) on GaSb (001) substrates (cut 2° towards [101]). Details of the OMVPE growth are given in Ref. 21. The optical data in the range of 0.75–5.3 eV [ultraviolet (UV)/visible (VIS)/near infrared (NIR)] was taken using an Instruments SA variable-angle ellipsometer. For the interval of 0.35–0.8 eV [midinfrared (MIR)/far infrared (FIR)], a variable-angle instrument which used a Fourier transform infrared reflectometer as a light source was employed. Thus, there was some overlap between the two intervals. The UV/VIS/NIR measurements were performed with a 70° incidence angle, and the MIR/FIR measurements were performed with 60° and 70° incidence angles. To remove the surface oxide, an etching procedure was performed on the UV/VIS/NIR ellipsometer with prealigned samples mounted vertically on a vacuum chuck in a windowless cell that maintained the surfaces in a dry-nitrogen atmosphere. The details of the etching procedure are given in Ref. 14, except in this study the etch was a 3:1 mixture of HCl: methanol followed by a quick rinse in methanol.

III. EXPERIMENTAL RESULTS

The solid lines in Figs. 1(a) and 1(b) are the experimental values of the real $[\epsilon_1(E)]$ and imaginary $[\epsilon_2(E)]$ components of the complex dielectric function, respectively, as a function of photon energy E for sample No. 1. The solid lines in Figs. 2(a) and 2(b) are the corresponding data for sample No. 2. In the ϵ_2 spectrum there is an absorption edge around 0.55 eV, doublet peaks in the range 2.0–2.5 eV, and a large feature with a peak around 4 eV, with some structure on the low-energy side around 3.5 eV. However, in contrast to Ref. 11 we observed a weak feature at around 1.2 eV.

The solid lines in Figs. 3(a) and 3(b) show the experimental values of $d\epsilon_1(E)/dE$ and $d\epsilon_2(E)/dE$, respectively, for sample No. 1 as obtained by taking the numerical derivative (with respect to E) of the solid curves in Figs. 1(a) and 1(b), respectively. The solid lines in Figs. 4(a) and 4(b) are the corresponding data for sample No. 2.

The experimentally determined real (n) (solid lines) and imaginary (κ) (dashed lines) components of the complex index of refraction for sample Nos. 1 and 2 are displayed in Figs. 5 and 6, respectively. In Figs. 7 and 8 we plot the

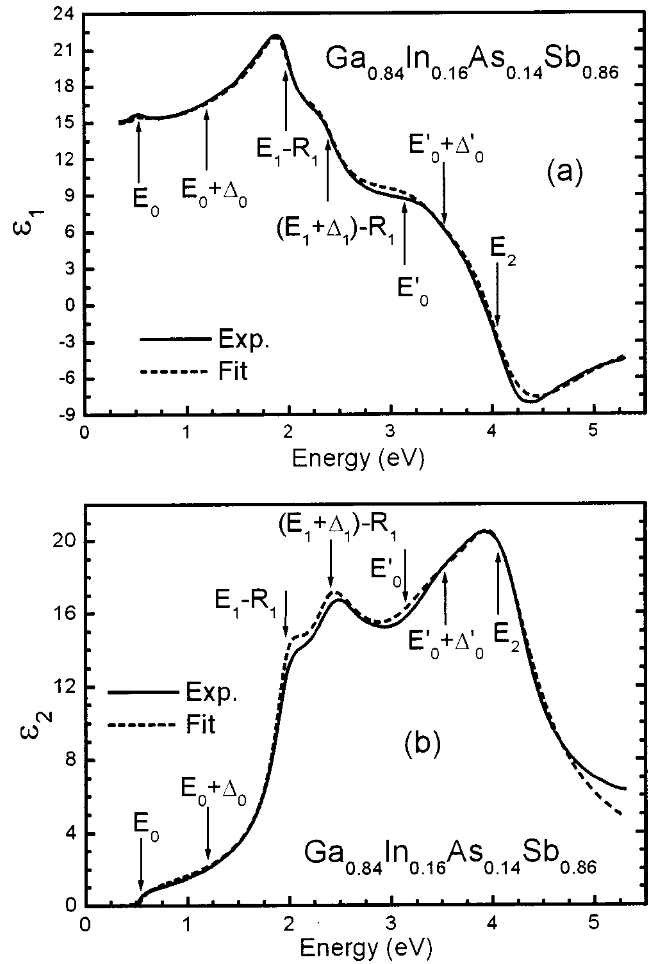

FIG. 1. Solid and dashed lines are the experimental and fit values, respectively, of the (a) real (ϵ_1) and (b) imaginary (ϵ_2) components of the complex dielectric function of GaInAsSb sample No. 1.

absorption coefficient α for sample Nos. 1 and 2, respectively. The insets of Figs. 7 and 8 show an expanded version of α in the region of the direct gap.

IV. THEORETICAL MODEL

In the direct-gap zinc-blende-type semiconductor GaInAsSb the spin-orbit interaction splits the highest-lying Γ_{15}^v valence band into Γ_8^v and Γ_7^v (splitting energy Δ_0) and the Γ_{15}^c conduction band into Γ_7^c and Γ_8^c (splitting energy Δ_0').[22] The corresponding lowest-lying transitions at $\mathbf{k}=0$ [three-dimensional (3D) M_0] are labeled $E_0[\Gamma_8^v(\Gamma_{15}^v)-\Gamma_6^c(\Gamma_1^c)]$ and $E_0+\Delta_0[\Gamma_7^v(\Gamma_{15}^v)-\Gamma_6^c(\Gamma_{11}^c)]$, respectively. The spin-orbit interaction also splits the $L_3^v(\Lambda_3^v)$ valence band into $L_{4.5}^v(\Lambda_{4.5}^v)$ and $L_6^v(\Lambda_6^v)$. The corresponding 2D M_0 CPs are designated $E_1[L_{4.5}^v(L_3^v)-L_6^c(L_1^c)$ or $\Lambda_{4.5}^v(\Lambda_3^v)-\Lambda_6^c(\Lambda_1^c)]$ and $E_1+\Delta_1[L_6^v(L_3^v)-L_6^c(L_1^c)$ or $\Lambda_6^v(\Lambda_3^v)-\Lambda_6^c(\Lambda_1^c)]$, respectively. The $E_0', E_0'+\Delta_0'$ features correspond to transitions from the Γ_8^v valence to the spin-orbit split Γ_7^c/Γ_8^c conduction levels and related transitions along ⟨100⟩.[22] The E_2 feature is due to transitions along ⟨110⟩ (Σ) or near the X point.[22]

The data near the E_0 band gap were fit to a function which contains Lorentzian-broadened (a) discrete excitonic (DE) and (b) 3D M_0 band-to-band continuum exciton BBCE

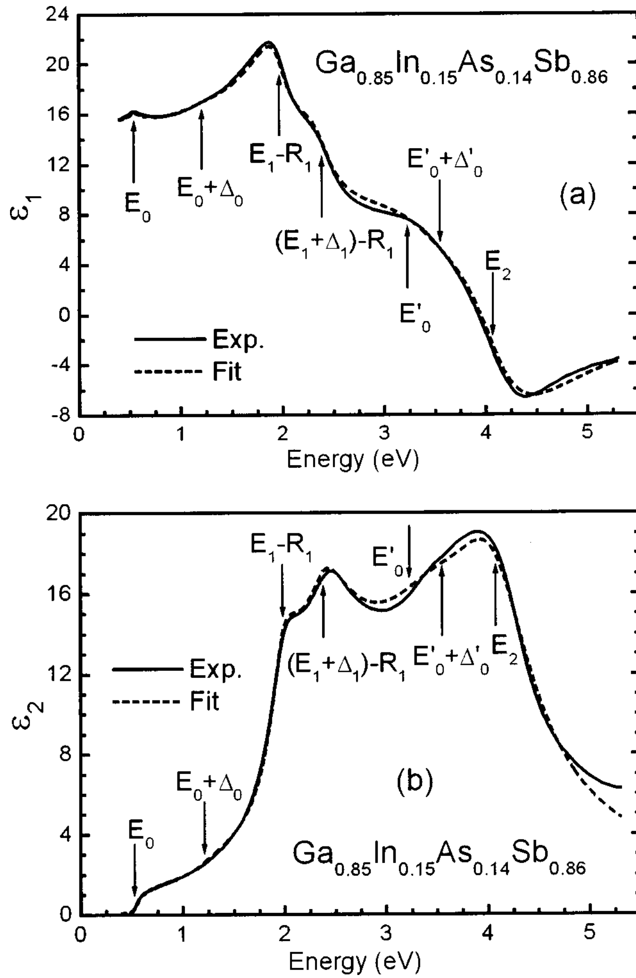

FIG. 2. Solid and dashed lines are the experimental and fit values, respectively, of the (a) real (ϵ_1) and (b) imaginary (ϵ_2) components of the complex dielectric function of GaInAsSb sample No. 2.

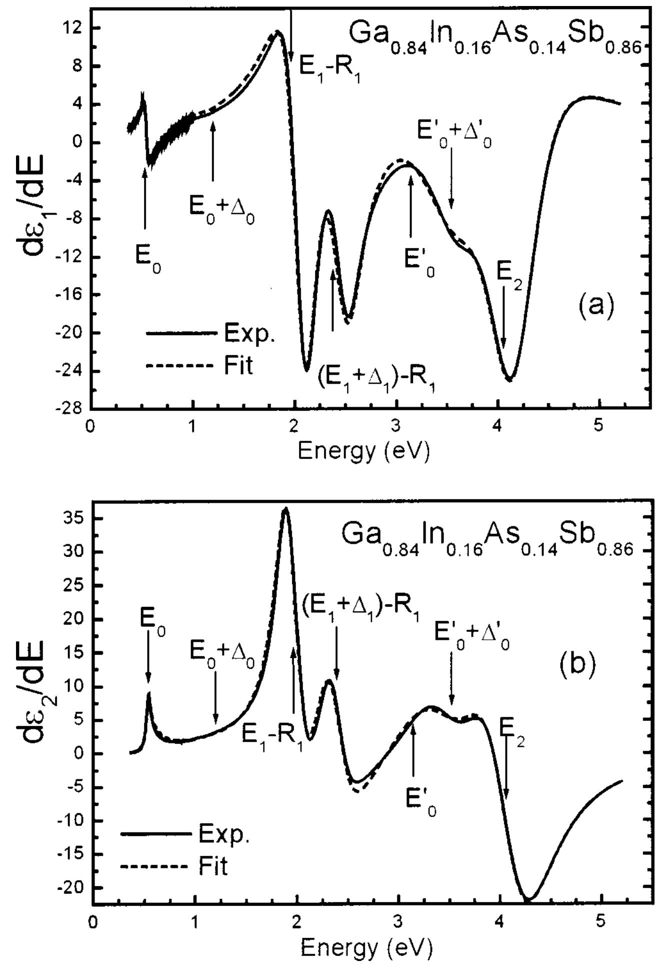

FIG. 3. Solid and dashed lines are the experimental and fit values, respectively, of (a) $d\epsilon_1/dE$ and (b) $d\epsilon_2/dE$ of GaInAsSb sample No. 1.

contributions. References 16, 23, and 24 have demonstrated that even if the E_0 exciton is not resolved, the Coulomb interaction still affects the band-to-band line shape. Thus, $\epsilon_2(E)$ is given by[14–17]

$$\epsilon_2(E)=\frac{A}{E^2}\left\{\mathrm{Im}\left\{\left[\frac{2R_0}{(E_0-R_0)-E-i\Gamma_0^{\mathrm{ex}}}+\frac{2R_0}{(E_0-R_0)+E+i\Gamma_0^{\mathrm{ex}}}\right]+\int_{-\infty}^{\infty}\left[\frac{\theta(E'-E_0)}{1-e^{-2\pi z_1(E')}}-\frac{\theta(-E'-E_0)}{1-e^{-2\pi z_2(E')}}\right]\frac{dE'}{E'-E-i\Gamma_0}\right\}\right\}, \quad (1)$$

where A is a constant, E_0 is the energy of the direct gap, R_0 is the effective Rydberg energy $[=(E_0-E_0^{\mathrm{ex}})],\Gamma_0^{\mathrm{ex}}$ is the broadening of the exciton, Γ_0 is the broadening parameter for the band-to-band transition, $z_1(E')=[R_0/(E'-E_0)]^{1/2}$, $z_2(E')=[R_0/(-E'-E_0)]^{1/2}$, and $\theta(x)$ is the unit step function. In Eq. (1) the quantity $A\propto(R_0)^{1/2}\mu_0^{3/2}|P_0|^2$, where μ_0 is the reduced interband effective mass at E_0, and P_0 is the matrix element of the momentum between Γ_8^v and Γ_6^c. The terms in the square brackets and under the integral in Eq. (1) correspond to the DE and BBCE (continuum exciton) contributions, respectively. Since the DE is not resolved, we take $\Gamma_0^{\mathrm{ex}}=\Gamma_0$.

For the $E_0+\Delta_0$ transition a function similar to Eq. (1) was used, with $A\rightarrow B$, $E_0\rightarrow E_0+\Delta_0$, $R_0\rightarrow R_{so}$, and $\Gamma_0\rightarrow\Gamma_{so}$.

For the E_1 CP, $\epsilon_2(E)$ is written as[14–17]

$$\epsilon_2(E)=\frac{C_1}{E^2}\left\{\mathrm{Im}\left\{\left[\frac{4R_1}{(E_1-R_1)-E-i\Gamma_{E_1}}+\frac{4R_1}{(E_1-R_1)+E+i\Gamma_{E_1}}\right]+\int_{-\infty}^{\infty}\left[\frac{\theta(E'-E_1)}{1+e^{-2\pi z_3(E')}}-\frac{\theta(-E'-E_1)}{1+e^{-2\pi z_4(E')}}\right]\frac{dE'}{E'-E-i\Gamma_{E_1}}\right\}\right\}, \quad (2)$$

where C_1 is a constant, E_1 is the energy of the gap, R_1 is the 2D Rydberg energy, Γ_{E_1} is the broadening parameter for both the exciton and band-to-band transition, $z_3(E')=[R_1/4(E'-E_1)]^{1/2}$, and $z_4(E')=[R_1/4(-E'-E_1)]^{1/2}$.

For the $E_1+\Delta_1$ CP, a function similar to Eq. (2) was used with $C_1\rightarrow C_2$ and $E_1\rightarrow E_1+\Delta_1$, $\Gamma_{E_1}\rightarrow\Gamma_{E_1+\Delta_1}$, etc. In practice, the same 2D Rydberg (R_1) was used for both the E_1 and $E_1+\Delta_1$ CP features.

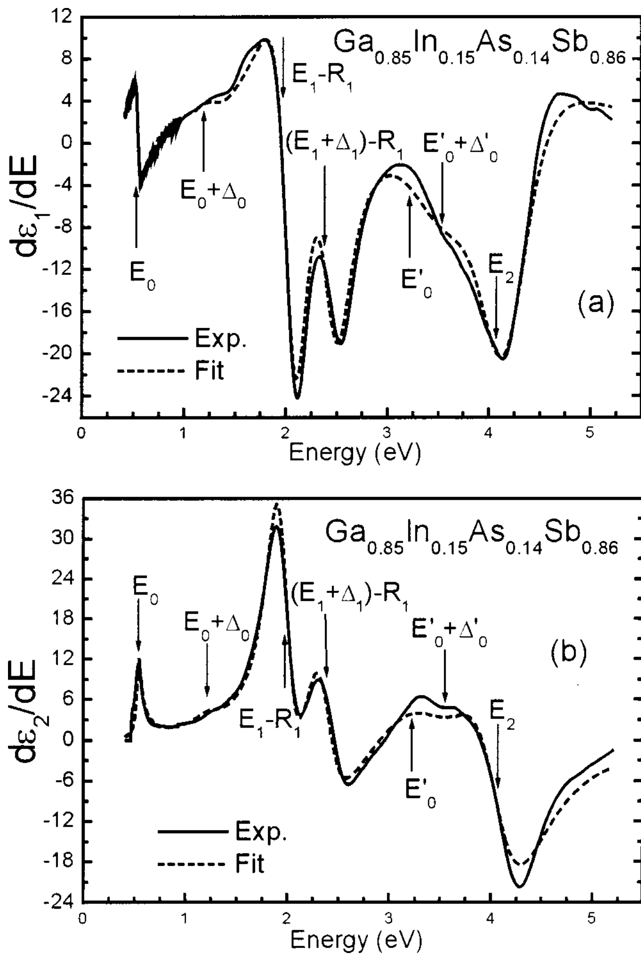

FIG. 4. Solid and dashed lines are the experimental and fit values, respectively, of (a) $d\epsilon_1/dE$ and (b) $d\epsilon_2/dE$ of GaInAsSb sample No. 2.

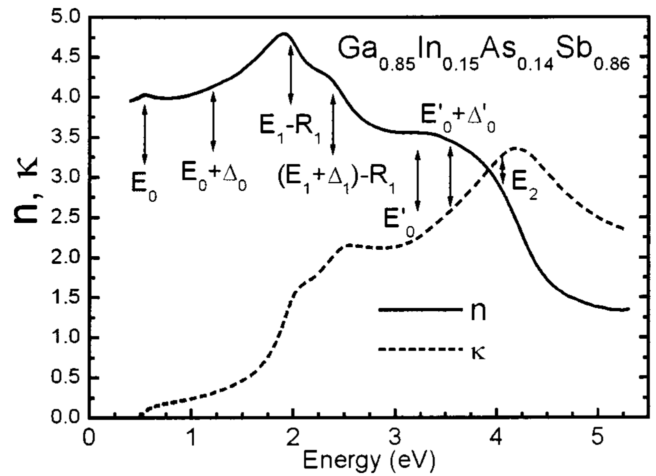

FIG. 6. Solid and dashed lines are the experimental values of the real (n) and imaginary (κ) components, respectively, of the complex index of refraction of GaInAsSb sample No. 2.

Reference 14 lists relatively simple analytical expressions for $\epsilon(E)$ for E_0, $E_0+\Delta_0$, E_1, and $E_1+\Delta_1$ based on the above equations.[25]

The nature of the E_0', $E_0'+\Delta_0'$, and E_2 features is more complicated in relation to $E_0/E_0+\Delta_0$ and $E_1/E_1+\Delta_1$ since the former do not correspond to a single, well-defined CP.[22] Therefore, each was described by a damped harmonic oscillator term:[17]

$$\epsilon(E)=\frac{F(j)}{[1-\chi^2(j)]-i\gamma(j)\chi(j)},\quad \text{with } j=E_0',\ E_0'+\Delta_0',\ \text{or } E_2, \tag{3}$$

where $F(j)$ is the amplitude, $\chi(j)=E(j)/E$, and $\gamma(j)$ is a dimensionless damping parameter.

The fact that Ref. 19 found that E_2, like the $E_0/E_0+\Delta_0$ and $E_1/E_1+\Delta_1$ CP features, contains an excitonic component provides some justification in using a damped oscillator term for this structure.

A constant $\epsilon_{1\infty}$ was added to the real part of the dielectric constant to account for the vacuum plus contributions from higher-lying energy gaps (E_1', etc.).[14–17] This quantity should not be confused with the high-frequency dielectric constant $\epsilon(\infty)$.

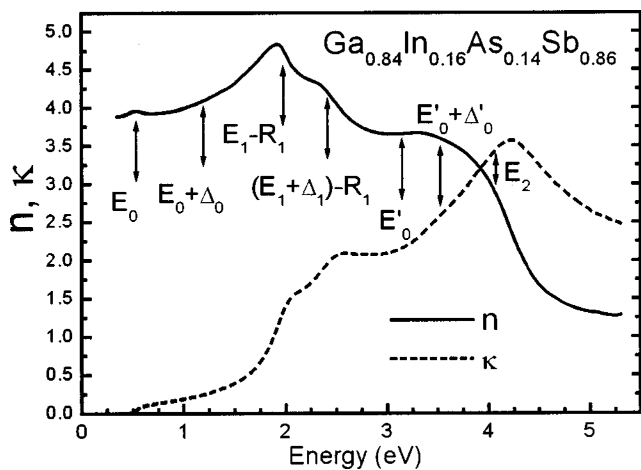

FIG. 5. Solid and dashed lines are the experimental values of the real (n) and imaginary (κ) components, respectively, of the complex index of refraction of GaInAsSb sample No. 1.

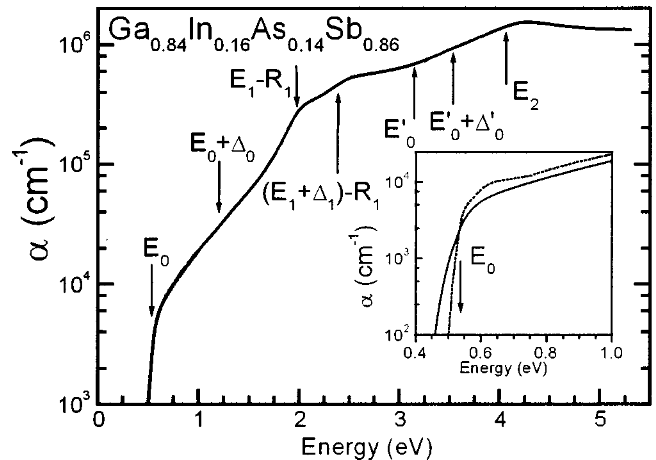

FIG. 7. Solid line is the experimental value of the absorption coefficient α for GaInAsSb sample No. 1. Solid and dashed lines in the inset show an expanded version of the experimental data and the linear interpolation of Eq. (7), respectively, in the region near E_0.

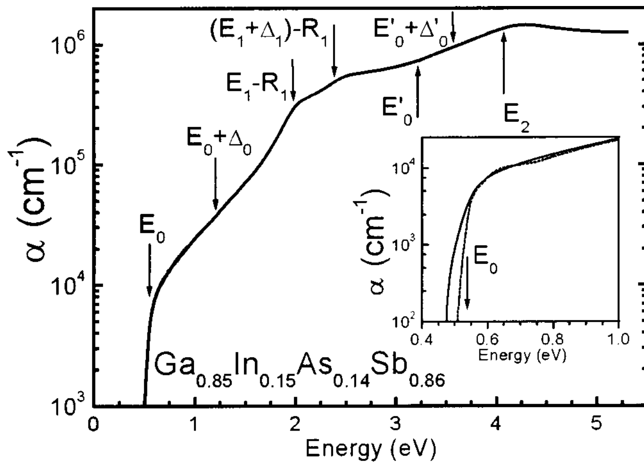

FIG. 8. Solid line is the experimental value of the absorption coefficient α for GaInAsSb sample No. 2. Solid and dashed lines in the inset show an expanded version of the experimental data and the linear interpolation of Eq. (7), respectively, in the region near E_0.

The dotted curves in Figs. 1(a), 1(b), 2(a), and 2(b) are fits to the experimental data using the above formulas. Since the exciton at $E_0/E_0+\Delta_0$ has not been resolved, a value of $R_0=1.2$ meV was estimated from R_0 of GaSb (1.6 meV) (Ref. 26) and effective-mass theory.[27] Because of the large number of fitting parameters, values for the various gaps and their broadening parameters were initialized from values obtained by numerically taking the first derivative of the dielectric functions (with respect to energy) and fitting to Eq. (A16) of Ref. 14. The details of this approach are given in Refs. 14–17. The final values of the different energies are indicated by arrows in the various figures. All relevant parameters are listed in Table I. The corresponding values of $d\epsilon_1(E)/dE$ and $d\epsilon_2(E)/dE$, obtained from Eq. (A16) of Ref. 14, are shown by the dotted lines in Figs. 3(a), 3(b), 4(a), and 4(b), respectively. Overall, there is very good agreement between experiment and theory for both the dielectric function [Figs. 1(a), 1(b), 2(a), and 2(b)] and the first derivative [Figs. 3(a), 3(b), 4(a), and 4(b)].

V. DISCUSSION OF RESULTS

The dependence of the direct gap of the quaternary $Ga_{1-x}In_xAs_ySb_{1-y}$ on composition at 300 K is given by[28]

$$E_{0,\mathrm{quat}(x,y)}=0.726-0.961x-0.501y+0.08xy+0.415x^2+1.2y^2+0.021x^2y-0.62xy^2, \quad (4a)$$

where for the condition of lattice matching to GaSb,[28]

$$y=\frac{0.867x}{1-0.048x}. \quad (4b)$$

Thus, from Eqs. (4a) and (4b) together with the values of E_0 listed in Table I, we find that sample Nos. 1 and 2 are $Ga_{0.84}In_{0.16}As_{0.14}Sb_{0.86}$ and $Ga_{0.85}In_{0.15}As_{0.14}Sb_{0.86}$, respectively. Therefore, these samples are very similar to the quaternary material in Ref. 11.

We estimated the value of R_0 listed in Table I for these quaternaries based on effective-mass theory and $R_0=1.6$ meV for GaSb.[26] The exciton binding energy can be expressed as[26]

$$R_0\propto\mu_0/\epsilon^2(\infty), \quad (5)$$

where μ_0 is the reduced interband effective mass at E_0 and $\epsilon(\infty)$ is the high-frequency dielectric constant.

The quantity $\epsilon(\infty)$ for the quaternaries can be estimated from a linear interpolation between the end-point binary materials given by Eq. (5) of Ref. 12. Using the values of the dielectric function of the binary end-point materials given in Ref. 12, we find $\epsilon(\infty)=14.1$ for our materials. This value is close to that of GaSb $[\epsilon(\infty)=14.4]$ since the main constituent of our samples is this binary.

Thus, the variation in R_0 is due mainly to differences in μ_0. For small-band-gap materials, μ_0 is dominated by the conduction-band effective mass m_c^*, and hence, from $\mathbf{k}\cdot\mathbf{p}$ theory[29]

$$R_0\propto m_c^*\propto\left[\frac{2}{E_0}+\frac{1}{E_0+\Delta_0}\right]^{-1}. \quad (6)$$

Thus, from the values of the relevant band gaps and R_0(GaSb) listed in Table I, we find R_0(quaternary) $=0.75R_0(\mathrm{GaSb})=1.2$ meV.

The absorption coefficient of the quaternaries in the region of the fundamental band gap $\alpha_{\mathrm{quat}(x,y)}(E)$ also can be estimated from a linear interpolation procedure given by[12,30]

$$\begin{aligned}\alpha_{\mathrm{quat}(x,y)}(E)=&xy\,\alpha_{\mathrm{InAs}}[E+E_{0,\mathrm{InAs}}-E_{0,\mathrm{quat}(x,y)}]+x(1-y)\\&\times\alpha_{\mathrm{InSb}}[E+E_{0,\mathrm{InAs}}-E_{0,\mathrm{quat}(x,y)}]+y(1-x)\\&\times\alpha_{\mathrm{GaAs}}[E+E_{0,\mathrm{GaAs}}-E_{0,\mathrm{quat}(x,y)}]+(1-x)\\&\times(1-y)\,\alpha_{\mathrm{GaSb}}[E+E_{0,\mathrm{GaSb}}-E_{0,\mathrm{quat}(x,y)}], \quad (7)\end{aligned}$$

where α_i and $E_{0,i}$ are the absorption coefficient and fundamental band gap of the relevant end-point materials (i = InAs, InSb, GaAs, or GaSb) and $E_{0,\mathrm{quat}(x,y)}$ is the fundamental band gap of the quaternary of composition *x,y*. Using the values of $E_{0,i}$ and absorption coefficients of InAs, InSb, and GaAs listed in Refs. 30 and 31, respectively, and $E_{0,\mathrm{GaSb}}(=0.724\,\mathrm{eV})$ and the GaSb absorption coefficient taken from Ref. 17, we obtain the dashed curves in the insets of Figs. 7 and 8. Due to alloy broadening, the experimental α is somewhat larger below the band gap in relation to the linear interpolation.

The measured values of ϵ_1 and ϵ_2 of this experiment are in good agreement with the corresponding data of Ref. 11. For comparison purposes, listed in Table I are the relevant parameters from this study. However, Snyder *et al.* did not model their data. Their values of ''$E_1/E_1+\Delta_1$'' and the corresponding broadening parameters listed in Table I were obtained by fitting the numerical second derivative of the data to an expression that corresponds to the second derivative of a 2D CP. This analysis is incorrect since the optical features associated with the $E_1/E_1+\Delta_1$ CPs are primarily excitonic.

Recently, Muñoz *et al.*[17] have measured the optical constants of GaSb in the range of 0.3–5.3 eV using SE. These

TABLE I. Values of the relevant parameters obtained in this experiment for the two GaInAsSb samples. Also listed are the room-temperature values of the PL peaks and some of the corresponding parameters for $Ga_{0.85}In_{0.15}As_{0.17}Sb_{0.83}$ and GaSb.

Parameter	Sample No. 1 ($Ga_{0.84}In_{0.16}As_{0.14}Sb_{0.86}$)	Sample No. 2 ($Ga_{0.85}In_{0.15}As_{0.14}Sb_{0.86}$)	$Ga_{0.85}In_{0.15}As_{0.17}Sb_{0.83}$ [a]	GaSb [b]
E_0 (eV)	0.535 ± 0.01 (0.538)[c]	0.542 ± 0.01 (0.555)[c]	0.55 ± 0.02	0.724 ± 0.005
A (eV^2)	0.034 ± 0.005	0.057 ± 0.005		0.10 ± 0.005
R_0, R_{so} (meV)	1.2[d]	1.2[d]		1.6
Γ_0, Γ_o^{ex} (meV)	22 ± 5	24 ± 5		15 ± 5
$E_0+\Delta_0$ (eV)	1.200 ± 0.03	1.205 ± 0.03		1.52 ± 0.02
B (eV^2)	0.020 ± 0.005	0.17 ± 0.005		0.20 ± 0.01
Γ_{so}, Γ_{so}^{ex} (meV)	120 ± 10	120 ± 10		15 ± 5
E_1-R_1 (eV)	1.976 ± 0.01	1.975 ± 0.01	1.971[e]	2.047 ± 0.003
C_1 (eV^2)	19.8 ± 0.01	19.7 ± 0.01		22.0 ± 0.007
R_1 (meV)	30 ± 5	30 ± 5		32 ± 3
Γ_{E_1}, $\Gamma_{E_1}^{ex}$ (meV)	150 ± 10	160 ± 10	88[f]	95 ± 5
$(E_1+\Delta_1)-R_1$ (eV)	2.39 ± 0.01	2.38 ± 0.01	2.421[g]	2.488 ± 0.005
$\Gamma_{E_1+\Delta_1}$, $\Gamma_{E_1+\Delta_1}^{ex}$	200 ± 15	195 ± 15	126[h]	220 ± 10
C_2 (eV^2)	24.8 ± 0.01	22.4 ± 0.01		30.0 ± 0.01
E_0' (eV)	3.14 ± 0.03	3.22 ± 0.03		3.40 ± 0.01
$F(E_0')$	0.03 ± 0.01	0.1 ± 0.01		1.20 ± 0.01
$\gamma(E_0')$	0.40 ± 0.05	0.45 ± 0.05		0.23 ± 0.01
$E_0'+\Delta_0'$ (eV)	3.53 ± 0.03	3.55 ± 0.03		3.79 ± 0.02
$F(E_0'+\Delta_0')$	2.37 ± 0.01	2.57 ± 0.01		1.03 ± 0.01
$\gamma(E_0'+\Delta_0')$	0.35 ± 0.05	0.40 ± 0.05		0.17 ± 0.01
E_2 (eV)	4.06 ± 0.01	4.07 ± 0.01		4.10 ± 0.005
$F(E_2)$	2.51 ± 0.01	2.11 ± 0.01		1.87 ± 0.01
$\gamma(E_2)$	0.22 ± 0.02	0.23 ± 0.02		0.125 ± 0.01
$\epsilon_{1\infty}$	2.39 ± 0.01	2.50 ± 0.01		1.97

[a]See Ref. 11.
[b]See Ref. 17.
[c]Room-temperature PL.
[d]Fixed.
[e]Incorrectly labeled E_1.
[f]$\Gamma_{E_1}^{ex}$.
[g]Incorrectly labeled $E_1+\Delta_1$.
[h]$\Gamma_{E_1+\Delta_1}^{ex}$.

data were also fit using the Holden model. For comparison purposes, Table I also lists the relevant parameters for GaSb obtained from this analysis. The absorption curves in the region of the direct gap for our quaternaries, as shown by the solid lines in the insets of Figs. 7 and 8, are very similar to the corresponding curve for GaSb near E_0,[17] although somewhat broader below the band gap due to alloy effects.

The optical constants ϵ_1 and ϵ_2 for GaSb,[17,32–34] and other diamond- and zinc-blende-type (DZB) semiconductors, over an extended range, have been investigated by a number of authors, mainly using SE.[14–17,35–42] However, Aspnes[32,40] and Cardona and co-workers[33,34] did not model their results, although the latter fit derivative spectra. In Ref. 42 Adachi used a model in which the E_0, $E_0+\Delta_0$, E_1, and $E_1+\Delta_1$ CPs are represented by only Lorentzian-broadened band-to-band single-particle (BBSP) expressions, i.e., no DE. As discussed below, the optical structure associated with the $E_1/E_1+\Delta_1$ CPs is primarily excitonic. In later works Adachi did include DE terms but with separate amplitude factors for the DE and BBSP contributions.[37,38] However, in the DE plus BBCE approach, for a given CP both terms must have the same strength parameter, e.g., $A(E_0)$ and $C_1(E_1)$, as indicated in Eqs. (1) and (2), respectively. In Paskov's treatment[23] the BBCE contribution is included at E_0, but not E_1.

The inadequacy of the BBSP approach at E_0 has been

clearly demonstrated in Refs. 16, 23, and 24. These works showed that in the region of the fundamental gap the BBCE term gave a better fit to experimental values of $d\epsilon_2/dE$ (Refs. 16 and 24) and α (Ref. 23) in relation to the BBSP expression. The deficiency of the BBSP model also is illustrated by Fig. 3 in Ref. 41. The fit expressions for the DE plus BBSP are considerably lower than the experimental data, particularly for the 20 K measurement. The effect of the BBCE term in relation to the BBSP expression is to both increase the oscillator strength and change the line shape from a 3D M_0 singularity to one that approximates a 2D M_0 function (within about 8–10 R_0 from E_0). Kim and Sivinathan[39] used DE plus BBSP terms with both Lorentzian and Gaussian broadening (increased fitting parameters). However, Aspnes found no evidence for Gaussian broadening based on a Fourier analysis of the optical constants of CdTe.[40]

Due to the relatively large values of $R_1(\approx 30-300\,\text{meV})$,[14–17] the optical structure associated with the $E_1, E_1+\Delta_1$ CPs in DZB semiconductors are actually mainly the excitonic features $E_1-R_1, (E_1+\Delta_1)-R_1$, respectively, as denoted in the figures. Almost all prior optical[11,32–42] and modulated[43,44] optical studies have incorrectly labeled these excitonic features as "$E_1, E_1+\Delta_1$."

Our values of $R_1(30\pm 5\,\text{meV})$ for the quaternary samples are in good agreement with that obtained experimentally for GaSb (Ref. 17) (see Table I) and in reasonable accord with a value of 25 meV deduced from effective mass/$\mathbf{k}\cdot\mathbf{p}$ theory. According to this approach[18]

$$R_1 \propto \mu_\perp/\epsilon^2(\infty), \tag{8a}$$

where $\mu_\perp$ is the perpendicular reduced interband effective mass related to E_1 and $\epsilon(\infty)$ is the high-frequency dielectric function. From a three-band $\mathbf{k}\cdot\mathbf{p}$ formula the perpendicular conduction ($m^*_{c,\perp}$) and valence ($m^*_{v,\perp}$) effective masses (in units of the free-electron mass) are given by

$$\frac{1}{m^*_{c,\perp}} = 1 + E_P\left(\frac{1}{E_1} + \frac{1}{E_1+\Delta_1}\right), \tag{8b}$$

$$\frac{1}{m^*_{v,\perp}} = 1 - \frac{E_P}{E_1}, \tag{8c}$$

where E_P is proportional to the square of the magnitude of the matrix element of the perpendicular momentum between the corresponding conduction and valence bands. Using the value of $E_P = 8.36\,\text{eV}$ for GaSb (Ref. 17) and the experimental values of E_1 and $E_1+\Delta_1$ deduced from Table I, $m^*_{c,\perp}$ and $m^*_{v,\perp}$ were determined from Eqs. (8b) and (8c), to obtain $\mu_\perp = 0.088$. For the quaternaries $\epsilon(\infty) = 14.1$, as discussed previously.

For CdTe, $R_1 = 145\,\text{meV}$, both experimentally[16] and from the considerations of Ref. 18. Therefore, using $\epsilon(\infty) = 7.05$ and $\mu_\perp = 0.15$ for CdTe (Ref. 26) and $\epsilon(\infty) = 14.1$, we find $R_1(\text{quaternary}) \sim 26\,\text{meV}$, in reasonably good agreement with our experimental number of $30\pm 5\,\text{meV}$.

The ability to measure R_1 has considerable implications for band-structure calculations, both empirical[22] and first principles.[19,20] In the former case, band-structure parameters, e.g., pseudopotential form factors, are determined mainly by comparison with optical and modulated optical experiments, including the "$E_1, E_1+\Delta_1$" features. Therefore, the band-to-band energies are too low by an amount R_1. Recently, Rohlfing and Louie published a first-principles calculation of the optical constants of GaAs, including excitonic effects.[19] Using this formalism they also calculated R_0. Their approach makes it possible to evaluate R_1 from first principles.[45] Albrecht *et al.* also have recently presented an *ab initio* approach for the calculation of excitonic effects in the optical spectra of semiconductors and insulators.[20] However, to date they have only presented results for Si.

VI. SUMMARY

In summary, we measured the room-temperature complex dielectric function of two epitaxial layers of GaInAsSb/GaSb in the extended range of 0.35–5.3 eV using spectral ellipsometry. Distinct structures related to critical points associated with the direct gap (E_0), spin-orbit split $E_0+\Delta_0$, spin-orbit split ($E_1, E_1+\Delta_1$) and ($E_0', E_0'+\Delta_0'$) doublets, and E_2 were observed. The $E_0+\Delta_0$ feature has not been reported in a previous SE investigation. The experimental data over the entire measured spectral range have been fit using the Holden model dielectric function based on the electronic energy-band structure near these CPs plus DE and BBCE effects at E_0, $E_0+\Delta_0$, E_1, and $E_1+\Delta_1$. The experimental absorption coefficients in the region of E_0 were in good agreement with values obtained from a linear interpolation of the end-point materials. In addition to measuring the energies of these various band-to-band CPs, we have evaluated the 2D exciton binding energy $R_1(=30\pm 5\,\text{meV})$, in good agreement with that of GaSb and in reasonable accord with effective mass/$\mathbf{k}\cdot\mathbf{p}$ theory. The ability to determine R_1 has important ramifications for recent first-principles band-structure calculations which have included excitonic effects at various critical points.

ACKNOWLEDGMENTS

Three of the authors (M.M., K.W., and F.H.P.) thank the National Science Foundation for Grant No. DMR-9414209 and the New York State Science and Technology Foundation through its Centers for Advanced Technology program for support of this project. One of the authors (M. M.) also acknowledges support from CONACyT, Mexican Agency through Research Project No. 25135E.

[1] G. W. Charache, J. L. Egley, D. M. Depoy, L. R. Danielson, M. J. Freeman, R. J. Dziendziel, J. F. Moynihan, P. F. Baldasaro, B. C. Campbell, C. A. Wang, H. K. Choi, G. W. Turner, S. J. Wojtczuk, P. Colter, P. Sharps, M. Timmons, R. E. Fahey, and K. Zhang, J. Electron. Mater. **27**, 1038 (1998).
[2] A. Andaspaeva, A. N. Baranov, and A. Gusseinov, Sov. Tech. Phys. Lett. **14**, 377 (1988).
[3] C. Caneau, A. K. Srivastava, A. G. Dentai, J. L. Zyskind, and M. A. Pollack, Electron. Lett. **21**, 815 (1985).
[4] A. E. Drakin, P. G. Eliseev, B. N. Sverdlov, A. E. Bochkarev, L. M. Dolginov, and L. V. Druzhinina, IEEE J. Quantum Electron. **23**, 1089 (1987).
[5] C. A. Wang and H. K. Choi, J. Electron. Mater. **26**, 1231 (1997); also, Appl. Phys. Lett. **70**, 802 (1997).
[6] R. J. Menna, D. R. Capewell, R. V. Martinelli, and P. K. York, Appl. Phys. Lett. **59**, 2127 (1991).

[7] H. K. Choi, J. N. Walpole, G. W. Turner, M. K. Connors, L. J. Missaggia, and M. J. Manfra, IEEE Photonics Technol. Lett. **10**, 938 (1998).
[8] M. F. Flatte, C. H. Grein, H. Ehrenreich, R. H. Miles, and H. Cruz, J. Appl. Phys. **78**, 4552 (1995).
[9] Y. Shi, J. H. Zhoa, J. Sarathy, H. Lee, and G. H. Olsen, IEEE Trans. Electron Devices **44**, 2167 (1997).
[10] K. Xie, J. H. Zhao, Y. Shi, H. Lee, and G. H. Olsen, IEEE Photonics Technol. Lett. **8**, 667 (1996).
[11] P. G. Snyder, T. E. Tiwald, D. W. Thompson, N. J. Ianno, J. A. Woollam, M. G. Mauk, and Z. A. Shellenberger, Thin Solid Films **313–314**, 667 (1998).
[12] A. Mezerreq, C. Linares, J. L. Lazzari, and A. Montaner, Thin Solid Films **221**, 196 (1992).
[13] A. G. Belov, A. I. Belogorokhov, A. E. Bocharev, L. M. Dolginov, L. V. Druzhinina, G. M. Zinger, M. A. Il'in, P. Yu. Karasev, M. G. Mil'vidskii, D. A. Rzaev, and A. I. Ryshkin, Sov. Phys. Solid State **26**, 84 (1984).
[14] T. Holden, P. Ram, F. H. Pollak, J. L. Freeouf, B. X. Yang, and M. C. Tamargo, Phys. Rev. B **56**, 4037 (1997).
[15] T. Holden, F. H. Pollak, J. L. Freeouf, G. W. Charache, J. E. Raynolds, and C. Geller, Proceedings of the 4th NREL Thermophotovoltaic Generation of Electricity Conference, Denver, Co, 1998, edited by T. J. Coutts, J. P. Brenner, and C. S. Allman, AIP Conf. Proc. **460** (AIP, Woodbury, NY, 1999), p. 39.
[16] K. Wei, F. H. Pollak, J. L. Freeouf, D. Shvydka, and A. D. Compaan, J. Appl. Phys. **85**, 7418 (1999).
[17] M. Muñoz, K. Wei, F. H. Pollak, J. L. Freeouf, and G. W. Charache, Phys. Rev. B **60**, 8105 (1999).
[18] Y. Petroff and M. Balkanski, Phys. Rev. B **3**, 3299 (1971).
[19] M. Rohlfing and S. G. Louie, Phys. Rev. Lett. **81**, 2312 (1998)
[20] S. Albrecht, L. Reining, R. Del Sole, and G. Onida, Phys. Rev. Lett. **80**, 4510 (1998).
[21] C. A. Wang, H. K. Choi, D. C. Oakley, and G. W. Charache, J. Cryst. Growth **195**, 346 (1998).
[22] M. L. Cohen and J. R. Chelikowsky, in *Electronic Structure and Optical Properties of Semiconductors* (Springer, Berlin, 1989).
[23] P. P. Paskov, J. Appl. Phys. **81**, 1890 (1997).
[24] F. H. Pollak, M. Muñoz, T. Holden, K. Wei, and V. M. Asnin, Phys. Status Solidi B **215**, 33 (1999).
[25] Equation (A13) in Ref. 14 should read $\xi^2(X)=4(E_1-X)/G$.
[26] *Numerical Data and Functional Relationships in Science and Technology*, Landolt-Börnstein edited by O. Madelung, M. Schultz, and H. Weiss, (Springer, New York, 1982), Vols. 17a and 17b.
[27] P. Y. Yu and M. Cardona, in *Fundamentals of Semiconductors: Physics and Materials Properties* (Springer, Berlin, 1996).
[28] J. C. DeWinter, M. A. Pollack, A. K. Srivatava, and J. L. Zyskind, J. Electron. Mater. **14**, 729 (1985).
[29] E. O. Kane, in *Semiconductors and Semimetals*, edited by R. K. Willardson and A. C. Beer (Academic, New York, 1966), Vol. 1, p. 75.
[30] S. Adachi, J. Appl. Phys. **61**, 4869 (1987).
[31] E. D. Palik, *Handbook of Optical Constants I* (Academic, New York, 1985); also, *Handbook of Optical Constants II* (Academic, New York, 1991).
[32] D. E. Aspnes and A. A. Studna, Phys. Rev. B **27**, 985 (1983).
[33] S. Zollner, M. Garriga, J. Humlicek, S. Gopalan, and M. Cardona, Phys. Rev. B **43**, 4349 (1991).
[34] M. Patrini, G. Guizzei, M. Galli, R. Ferrini, A. Bosacchi, S. Franchi, and R. Magnanini, Solid State Commun. **101**, 93 (1997).
[35] F. H. Pollak, in *1967 International Conference on II–VI Semiconducting Compounds*, edited by D. G. Thomas (Benjamin, New York, 1967), p. 552.
[36] P. Lautenschlager, M. Garriga, S. Logothetidis, and M. Cardona, Phys. Rev. B **35**, 9174 (1987); P. Lautenschlager, M. Garriga, and M. Cardona, *ibid.* **36**, 4813 (1987).
[37] S. Adachi, T. Kimura, and N. Suzuki, J. Appl. Phys. **74**, 3435 (1993); S. Adachi and T. Taguchi, Phys. Rev. B **43**, 9569 (1991).
[38] K. Suzuki and S. Adachi, J. Appl. Phys. **83**, 1018 (1998).
[39] C. C. Kim and S. Sivinathan, J. Appl. Phys. **78**, 4003 (1995); also, Phys. Rev. B **53**, 1475 (1996).
[40] D. E. Aspnes, Sol. Energy Mater. Sol. Cells **32**, 413 (1994).
[41] S. Adachi, Phys. Rev. B **41**, 1003 (1990).
[42] S. Adachi, J. Appl. Phys. **66**, 6030 (1989).
[43] M. Cardona, in *Modulation Spectroscopy* (Academic, New York, 1969).
[44] F. H. Pollak and H. Shen, Mater. Sci. Eng., R. **10**, 275 (1993).
[45] S. G. Louie (private communication).